

Vesicle Shapes from Molecular Dynamics Simulations

A. J. Markvoort,^{*,†,‡} R. A. van Santen,[‡] and P. A. J. Hilbers[†]

Department of Biomedical Engineering, TU Eindhoven, Postbus 513, 5600 MB Eindhoven, The Netherlands, and Department of Chemical Engineering, TU Eindhoven, Postbus 513, 5600 MB Eindhoven, The Netherlands

Received: July 31, 2006

Lipid bilayer membranes are known to form various structures such as large sheets or vesicles. When the two leaflets of the bilayer have an equal composition, the membrane preferentially forms a flat sheet or a spherical vesicle. However, a difference in the composition of the two leaflets may result in a curved bilayer or in a wide variety of vesicle shapes. Vesicles with different shapes have already been shown in experiments and diverse vesicle shapes have been predicted theoretically from energy minimization of continuous curves. Here we present a molecular dynamics study of the effect of small changes in the phospholipid headgroups on the spontaneous curvature of the bilayer and on the resulting vesicle shape transformations. Small asymmetries in the bilayers already result in high spontaneous curvature and large vesicle deformations. Vesicle shapes that are formed include ellipsoids, discoids, pear-shaped vesicles, cup-shaped vesicles, as well as budded vesicles. Comparison of these vesicles with theoretically derived vesicle shapes shows both resemblances and differences.

1. Introduction

Vesicles are highly adaptive structures having a rich diversity of shapes. One of the reasons for shape change is a difference in composition of the two leaflets of the vesicle membrane. Tanaka et al.¹ found that giant unilamellar vesicles (GUVs) of dipalmitoylphosphatidylcholine (DPPC)/cholesterol membranes undergo shape changes when lysophosphatidylcholine (lyso-PC) is added to the aqueous solution. Above the threshold concentration in water, the lyso-PC dissolves in the external monolayer. Because the flip-flop rate of lyso-PC in such membranes is low compared to the time scale of the shape transition, the lyso-PC does not reach the inner monolayer. The resulting difference in composition between the inner and outer monolayer results in an imbalance of the membrane, which is decreased by a shape transition (in this case bud formation) of the vesicle.

An older example of an experimental study of vesicle shape changes is by Käs and Sackmann² who studied shape changes of dimyristoylphosphatidylcholine (DMPC) and palmitoyl-oleylphosphatidylcholine (POPC) vesicles in ion-free water. The outer solution of an DMPC vesicle swollen in inositol was slowly exchanged by dialysis against a NaCl solution with equal osmolarity. This resulted in a shape change from an ellipsoid to a cup. The explanation given was that the inositol molecules are dissolved in the two monolayers of the vesicle. The decrease of inositol concentration at the outside results in a decrease of the amount of inositol molecules in the outer monolayer, resulting in an asymmetry between the two monolayers. This difference in composition between the inner and outer monolayer results again in an imbalance of the membrane, which is once more solved by a shape change, which in this case resulted in the formation of a cup-shaped vesicle.

A number of theoretical models explaining the different vesicle shapes exist: the spontaneous curvature model,³ the

bilayer coupling model,^{4,5} and the area-difference elasticity (ADE) model.⁶ Applied to vesicles, these models, which describe the membrane as a continuum, predict a wide variety of vesicle shapes.^{7,8} In the experimental studies described above, GUVs are investigated using various microscopical approaches. New microscopical approaches, such as two-photon microscopy, result in increasingly detailed visualization^{9,10} of the process, but the membranes remain visible only as a continuous medium, as in theoretical models. Contrarily, using molecular dynamics computer simulations, the process can be studied at a molecular level for smaller unilamellar vesicles (SUVs).

Here, we study the influence of small changes in the phospholipid headgroups on bilayer curvature and on vesicle shapes using such molecular dynamics simulations. For these simulations, we use the same coarse grained lipid model that we have used before to study the spontaneous formation of vesicles and the bilayer-vesicle transition¹¹ as well as the fusion of such vesicles.¹² These simulations show that small changes of the headgroups can be related to a spontaneous curvature of the bilayer and that by such small changes of the headgroups a wide variety of vesicle shapes can be obtained. Furthermore, the vesicle shapes obtained by the simulations are compared with vesicle shapes predicted by the theoretical models.

2. Lipid Model

The molecules used in this coarse grained study are shown in Figure 1. Figure 1a shows the van der Waals representation of dipalmitoylphosphatidylcholine (DPPC), a typical example of the glycerophospholipids class on which our coarse grained (CG) lipids (Figures 1b and 1c) are based. In our prior vesicle formation and fusion studies^{11,12} only one type of lipid was used. The spontaneously formed bilayers were flat and the spontaneously formed vesicles spherical, as expected for symmetric bilayers. To introduce asymmetry in the bilayers, we here use two types of lipids instead of only one. The difference between the two lipid types is their slightly different headgroup parameters. Hence, in our CG model now three types of coarse

* Corresponding author. E-mail: A.J.Markvoort@tue.nl.

[†] Department of Biomedical Engineering.

[‡] Department of Chemical Engineering.

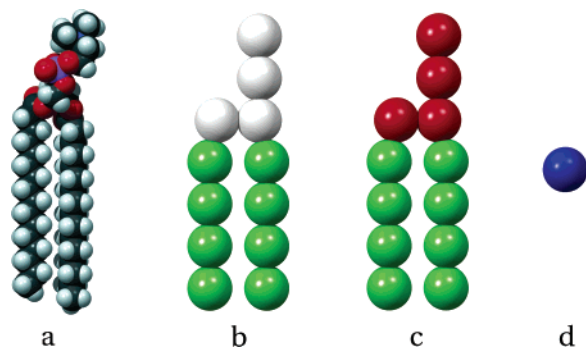


Figure 1. van der Waals representation of (a) dipalmitoylphosphatidylcholine (DPPC), (b) our coarse grained lipid type A, (c) lipid type B, and (d) water. All particles are colored corresponding to their type using a color scheme that is employed throughout the whole article. The difference between our two lipid types are small changes in the headgroup parameters.

grained particles are used to describe the chemically relevant groups in the phospholipids. The apolar tails of both phospholipids are represented by T particles, whereas for the polar headgroups two different headgroup particles are used. For the lipid in Figure 1b, which will be referred to in the remainder of the text as lipid A, the headgroup is represented by HA particles. The other lipid type, shown in Figure 1c and which will be denoted further as lipid B, the headgroup is formed of HB particles. To simulate phospholipid–water mixtures, a fourth particle type W (Figure 1d) is present in our CG model which makes up the solvent (water). For the derivation of the interaction parameters and the force fields used we refer to ref 11. The only difference in the lipids is a small change in the headgroup–headgroup and headgroup–water interaction parameters. These changes can resemble a different lipid, e.g., DPPE instead of DPPC, or be due to different environments, e.g., a different pH or different (concentration of) ions at both sides of a bilayer. Since we do not intend to study one particular mixture of lipids or specific ion concentrations and pH, but instead want to study both the phenomena and how large changes in the headgroups should be in order to have notable effect on the bilayers, we have chosen the following scheme of adapting the interaction parameters. Compared to the parameters from the prior simulations the headgroup–headgroup interaction for lipid type A has been decreased with a percentage and the headgroup–water interaction increased with the same percentage. For the other lipid type (lipid type B), the changes are reversed, i.e., an increase of the headgroup–headgroup interaction and a decrease of the headgroup–water interaction, again with the same percentage. To obtain domain/raft formation, the mutual interaction between headgroups of different types has been decreased (to $\epsilon = 1.5$) such that the two lipid types phase-separate.

All simulations have been performed using our in-house developed molecular dynamics program PUMMA. For the initial configurations of the simulations, spontaneously formed structures from randomly dispersed lipids of one type have been taken. Part of these lipids are then assigned type A and the other part type B.

3. Spontaneous Curvature in Bilayers

First we study the influence of having two different types of lipids with slightly changed headgroup–headgroup and headgroup–water interactions on periodic bilayers.

3.1. Simulation Results. Simulations have been performed on a system of size $21 \times 21 \times 10 \text{ nm}^3$ containing 512 lipids of

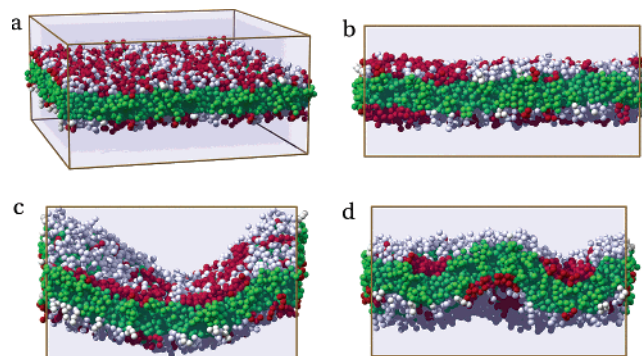


Figure 2. Spontaneous curvature in a bilayer due to two types of lipids of which only the headgroups differ slightly. (a) Overview of the initial configuration where the two types of lipids are randomly distributed, (b) side view of the resulting bilayers for 0% change in the parameters, i.e., identical parameters for lipids A and B, (c) 5% change in the parameters, and (d) 10% change in the parameters.

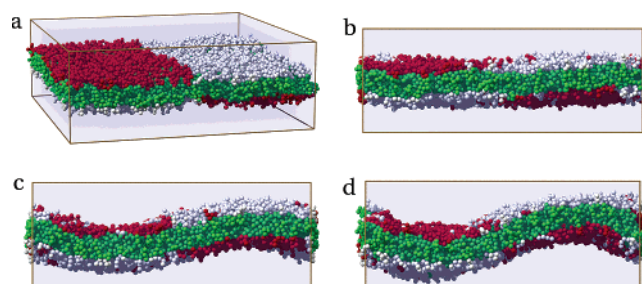


Figure 3. Spontaneous curvature in a bilayer with larger domains. (a) Overview of initial configuration, (b) side view of the resulting bilayers for 0% change, (c) 1.25% change, and (d) 2.5% change in the headgroup parameters, respectively.

type A, 512 lipids of type B, and 25 884 water particles. Initially, the lipids of the two types were randomly distributed over the bilayer as shown in Figure 2a. As in ref 11 for only one lipid type, the control simulation with 0% change in the parameters (Figure 2b) results in a flat bilayer with small oscillations, although domain/raft formation occurs. In parts c) and d) of the same figure, results are shown for 5% and 10% change in the parameters, respectively.

Notice the opposite positioning of the domains in the upper and lower layer relative to each other in the curved bilayers. Domains of lipids of one lipid type in the upper monolayer coincide with domains of the other lipid type in the lower monolayer. In this way a spontaneous curvature is introduced in the bilayer.

In Figure 3 the same phenomenon is shown, but now for larger domains and smaller parameter changes. In these simulations, 1024 lipids of type A and 1024 lipids of type B have been distributed initially such that there are only two domains (Figure 3a). In the left half of the bilayer, the lower monolayer consists of lipids of type A and the upper monolayer of lipids of type B. In the right half of the bilayer this is exactly the other way around, such that two domains with opposite curvature are formed. Apart from the 2048 lipids, the simulation box with initial size $30 \times 30 \times 11 \text{ nm}^3$ contains 56 997 water particles. Again, the control simulation with identical parameters for lipids A and B (Figure 3b) remains a flat bilayer, whereas small changes, i.e., 1.25% change (Figure 3c) and 2.5% change (Figure 3d), already result in a highly curved bilayer. Here again, the domains in the upper and lower monolayer of opposite type remain coinciding for the curved bilayers (Figure 3c and d), whereas they can shift relative to each other for the flat bilayer (Figure 3b).

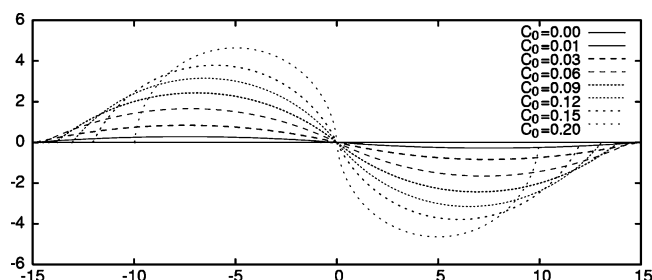


Figure 4. Curve with minimum energy for various values for the spontaneous curvature C_0 .

This figure shows that for larger domains even small changes in the headgroup parameters result in a stable curved bilayer.

3.2. Comparison with Spontaneous Curvature Model. To determine the relation between the change in our interaction parameters and the spontaneous curvature of these bilayers, we compare the bilayers from Figure 3 with predictions for membrane shapes from continuum models. The first of these methods is the spontaneous curvature model.⁷ The main idea of this spontaneous curvature model is that the shape of a membrane can be predicted by calculating the shape with the minimum bending energy for the membrane, where this bending energy is given by

$$E_b = \int_A \left[\frac{k_c}{2} (C_1(a) + C_2(a) - C_0)^2 + \frac{\bar{k}_c}{2} C_1(a) C_2(a) \right] da \quad (1)$$

where k_c and \bar{k}_c are elasticity constants and C_1 and C_2 the two principal curvatures. Further, the phenomenological parameter C_0 is the spontaneous curvature, i.e., the curvature of a membrane in its state of lowest elastic energy. This spontaneous curvature is 0 for a symmetric, hence flat, bilayer. But it will be nonzero for a bilayer with a built-in asymmetry.

Since the curvature in the bilayers is expected only in one dimension due to the partitioning of our bilayers in one-half with lipids of type A and the other with lipids of type B on top, C_2 equals 0, and as a consequence eq 1 reduces to

$$E_b = \frac{k_c}{2} W \int_0^L (C_1(s) - C_0)^2 ds \quad (2)$$

where W is the width of the membrane perpendicular to the direction in which it bends. Curves with minimum energy for various values of the spontaneous curvature C_0 have been calculated by minimizing this energy functional under the constraint of a fixed curve length. In the second half of the curve the implied spontaneous curvature C_0 is minus the value of the first half. The resulting curves are shown in Figure 4 for a curve of 30 nm length and various values for the spontaneous curvature.

From comparison of the curves with the bilayers (as in Figure 5), it follows that 0% change in interaction parameters results in zero spontaneous curvature, 1.25% change in interaction parameters in an approximate spontaneous curvature of 0.045 nm⁻¹, and a 2.5% change in a spontaneous curvature of 0.09 nm⁻¹.

4. Vesicle Shape Dependence on Spontaneous Curvature

A difference in interaction parameters between the two monolayers thus results in spontaneous curvature of bilayers. In case the bilayer forms a vesicle, such a spontaneous curvature of the bilayer will influence the shape of that vesicle as well. By using one type of lipid in the inner monolayer and the other

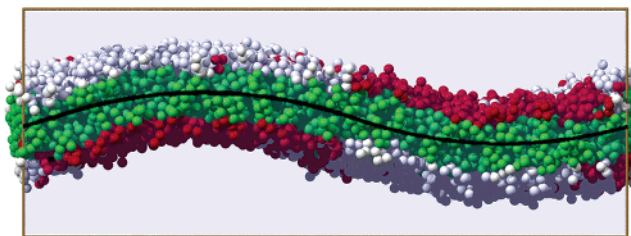


Figure 5. Overlay of a bilayer with a 1.25% change in the parameters with the solution of the spontaneous curvature model for $C_0 = 0.045$ nm⁻¹ (black line).

type in the outer monolayer of a vesicle, this influence of the spontaneous curvature on the vesicle shape is studied.

4.1. Simulation Results. For these simulations we could start from a spontaneously formed vesicle. However, such a vesicle is spherical and will remain spherical, as for a sphere hardly any shape changes are possible without changing the interior volume. In our simulations, the volume of a vesicle can hardly change, since diffusion of water through the membrane is slow compared to the simulation times reachable with our molecular dynamics simulations.¹³

Therefore, we start from a vesicle that was formed by the fusion of two smaller vesicles.¹² This vesicle, which is shown in Figure 6c, consists of 2048 lipids, of which 1289 lipids form the outer and the remaining 759 lipids the inner monolayer. The spontaneous curvature is introduced by using lipids of type A for the outer monolayer and lipids of type B for the inner monolayer. Apart from these 2048 lipids, the simulation box with initial size 30 × 30 × 41 nm³ contains 276 080 water particles, of which 7009 are in the vesicle interior. Because the vesicle was formed by the fusion of two smaller spherical vesicles, which have a smaller volume-to-area ratio than larger spherical vesicles, and because the water permeability is low, the vesicle does not contain enough water to be spherical and is elongated instead. Because the interior volume is less than that of a spherical vesicle, this vesicle is able to form many different shapes of which the one with the lowest free energy is most likely to occur. Here we study the shapes that are formed as a function of the spontaneous curvature by changing the headgroup interaction parameters. Simulations have been performed with steps of 2.5% in the range from -10% to 5% parameter change. A negative change means that the preferred curvature of the bilayer is concave, thus opposite to the curvature that is necessary for a spherical vesicle, whereas a positive change results in a preferential convex membrane. Each run consists of 5 000 000 iterations, taking 11 days of computer power when using 20 processors of our AMD Opteron 1 GHz Linux cluster.

The results shown in Figure 6 display a wide variety of shapes. In the order from low (most negative) to high preferred curvature, cup-shaped, discoid, prolate ellipsoid, pear-shaped, and budded vesicles are formed. All mentioned shapes from 0% to 5% parameter change are stable, i.e., once formed they persist for the remainder of the simulation. Also a -2.5% parameter change, which is not shown in the figure, resulted in a stable prolate ellipsoid. However, a change of -5% did not result in a stable end shape. Instead, the vesicle kept changing its shape between a prolate ellipsoid (as in Figure 6c) and a discoid (as in Figure 6b), indicating that it is exactly on the border between these two regimes. The discoid formed for a -7.5% parameter change is again stable. Finally, the cup-shape form in Figure 6a is again unstable. When the simulation is

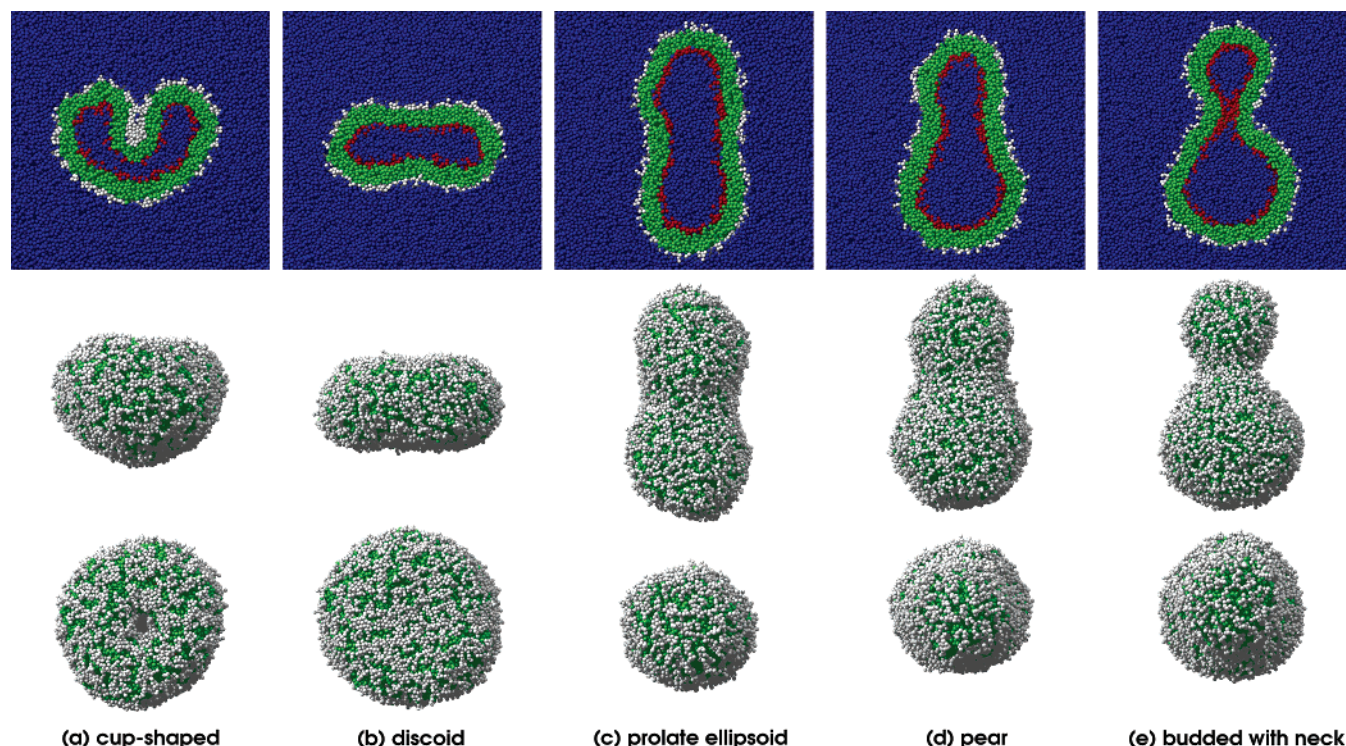


Figure 6. Vesicle shape as a function of the spontaneous curvature by changing headgroup parameters: (a) -10% , (b) -7.5% , (c) 0% , (d) 2.5% , and (e) 5% . For each of these vesicles, a cross-section through the vesicle center and parallel to its rotation axis is shown in the top row, a side view in the middle row, and a top view in the bottom row.

continued, the cup further closes until the opening at the top closes by a fusion of the contacting parts of the outer membrane monolayer.

4.2. Comparison with Spontaneous Curvature Model. The relation between the change in our interaction parameters and the resulting spontaneous curvature that we found for the periodic bilayers can now be used to compare our vesicle shapes with shapes predicted by the spontaneous curvature model. In a phase diagram of this model, the relevant parameters are the volume fraction ν and the reduced spontaneous curvature c_0 . The volume fraction ν is defined as the actual volume of a vesicle divided by the volume of a spherical vesicle with the same membrane area. The radius of this spherical vesicle with the same membrane area is denoted by R_0 and the reduced spontaneous curvature c_0 is then defined as $c_0 = C_0 R_0$.

As described in the simulations section, the initial configurations of our vesicle simulations were formed by the fusion of two vesicles. Each of these vesicles had a radius R_s of 4.6 nm and thus a volume $V_s = (4/3)\pi R_s^3 = 4.0 \times 10^2 \text{ nm}^3$. By the fusion of two such vesicles, both the membrane area and the interior volume are doubled. Considering just the membrane area, a spherical vesicle with a radius $\sqrt{2}$ times the original vesicle radius R_s can be formed. This radius, R_0 , thus equals approximately 6.5 nm. As the interior volume of such a spherical vesicle would be $2^{3/2}$ times the volume of one of the original vesicles, the volume fraction for the fused vesicle is $\nu = 1/\sqrt{2} \approx 0.71$. Therefore, in Figure 7a the solutions of the spontaneous curvature model with minimum energy, which we solved using the method as described by Seifert et al.,⁸ are shown as a function of the reduced spontaneous curvature c_0 for a vesicle with this volume fraction $\nu = 0.71$.

To compare these vesicle shapes with the shapes found in our simulations, we use the relation between C_0 and the parameter changes found for the periodic bilayer. From the simulations of the bilayers we found that a 2.5% change in the

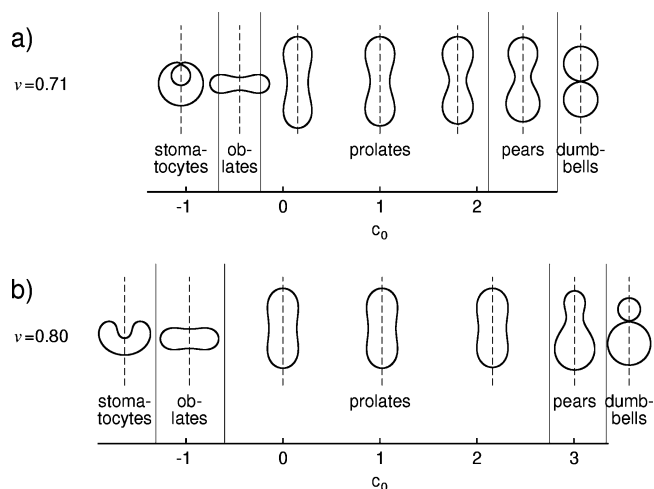


Figure 7. Shapes with minimal curvature energy as a function of the spontaneous curvature for two different volume fractions (a) $\nu = 0.71$ and (b) $\nu = 0.80$.

interactions yields a spontaneous curvature $C_0 = 0.09 \text{ nm}^{-1}$. For our vesicles, for which R_0 equals 6.5 nm, this results in $c_0 = C_0 R_0 = 0.6$. Analogously, for a 5% change this yields $c_0 = 1.2$. Extrapolating the relation between the parameter change and the spontaneous curvature linearly, further yields $c_0 = -1.8$ for -7.5% change and $c_0 = -2.4$ for 10% change.

The values obtained in this way for the spontaneous curvatures can be compared to the theoretically predicted value ranges for which the same shapes occur (ref 7 as depicted in Figure 7a). This shows that the shapes appear in the same order with increasing spontaneous curvature, but that there is an offset in c_0 of approximately 1.5 and that the shapes are slightly different. The offset can be explained by the fact that the two original vesicles that fused to form the initial configuration were formed spontaneously. As a result, the bilayer has fewer lipids in its inner monolayer than in its outer monolayer, such that the bilayer

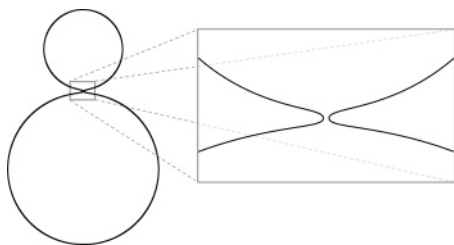


Figure 8. Budded vesicle according to the spontaneous curvature model. At the left the whole vesicle is shown and at the right has been zoomed in at the neck, showing the high curvature predicted by the continuum models which cannot be present in membranes with an apparent thickness as is the case in our simulations.

fits the curvature of that vesicle. Thus, there is not only spontaneous curvature because of the changed interaction parameters but also from the intrinsic unequal distribution of lipids between the inner and outer monolayer. The radius of the original vesicle is R_s , and thus the originally present curvature equals $1/R_s$. Since R_0 for the fused vesicle is $\sqrt{2}R_s$, the resulting offset in C_0R_0 equals $\sqrt{2}$. This offset indeed makes our simulations overlap with the regions from the spontaneous curvature model.

The fact that the shapes from the simulations are slightly different from the theoretically predicted shapes can be accounted for by a number of reasons. In the first place, the thickness of our membranes is not negligible as is the case in the theoretical models. The effect of the membrane thickness can be seen best for the budded vesicle as shown in Figure 8.

The high curvature bend in the theoretical model cannot occur in the simulations due to the membrane thickness. Because part of the membrane is then needed to form the neck between the two vesicles, less membrane area remains to envelop the vesicle interior, leading to a higher volume fraction. Hence, the membrane thickness influences the shapes in such a way that the simulation shapes look more like shapes predicted theoretically for a higher volume fraction, e.g., $v = 0.80$ for which the shapes are shown in Figure 7b.

A second important reason is that changing the headgroups of the lipids will also influence the packing of the lipids in the bilayer and thus can also alter the membrane area and as such the volume fraction. Furthermore, because the vesicles in our simulations are small, the curvatures are relatively high. As the elasticity constant k_c in the spontaneous curvature model might be not constant for high curvature, this can also influence the shape. Namely, if k_c increases for high curvature, structures which lack regions with high curvature are more favorable. A fourth source for differences between the theoretical shapes and our simulations originates from the dynamics. Namely, our shapes are not completely constant, but small undulations due to thermal oscillations are always present.

4.3. Comparison with Other Continuum Models. Besides the spontaneous curvature (SC) model that we used so far for comparison, two more continuum models are used, namely the bilayer coupling (BC) model⁴ and the area-difference elasticity (ADE) model.⁶ The main idea of all these models is that the shape of a membrane can be predicted as a function of some parameters by calculating the shape with the minimum energy for the membrane subject to constraints on the enclosed volume V and the membrane surface area A . For the area-difference elasticity model, this energy is given by

$$E_b = \int_A \frac{\kappa}{2} (C_1(a) + C_2(a) - C_0)^2 da + \frac{\bar{\kappa}}{2} \frac{\pi}{AD^2} (\Delta A - \Delta A_0)^2 \quad (3)$$

where κ and $\bar{\kappa}$ are elasticity constants and C_1 and C_2 again the two principal curvatures, and C_0 the spontaneous curvature. Furthermore, D is the bilayer thickness, ΔA the area difference between the inner and outer monolayer and ΔA_0 the preferred area difference based strictly on the number of lipid molecules it contains. This ADE model has been developed as a compromise between the other two models and reduces to the SC model for $\bar{\kappa}/\kappa \rightarrow 0$ and to the BC model for $\bar{\kappa}/\kappa \rightarrow \infty$.

As observed by Svetina and Zeks,⁵ the spontaneous curvature model and the bilayer coupling model can be rewritten into each other, leading to the same shape equations, which we solved using the method as described by Seifert, et al.⁸ Also the third model, which is a compromise between the former two models, results in the same shape equations.

All models thus have the same shape equations, but differ in the parameters used and the energy formula that is minimized. As a result, each model will have a different phase diagram and one model will be better in describing transitions in this phase diagram from one vesicle shape to the other, whereas the overall behavior is the same. However, as shown in section 3.2, the relation between the changes in our interaction parameters and the spontaneous curvature C_0 could be made straightforward. But for other parameters in the models, such as ΔA_0 , this is more difficult because areas are difficult to measure accurately for our small vesicles. The precise definition of the area, e.g., which of the headgroup particles do we consider and how smooth should the surface area be, influences the result. Such inaccuracies in the determination of areas result in even larger inaccuracies in differences of areas, such as both ΔA_0 and ΔA , and will make comparison with the models unreliable as small differences between ΔA_0 and ΔA already yield quite large differences in the predicted shapes.

In all simulations discussed so far, spontaneous curvature has been introduced by changing the parameters of both lipid types. But spontaneous curvature can also arise when only the interaction parameters for one lipid type are changed. Then approximately twice as large changes are necessary to obtain the same spontaneous curvature in the membrane.

5. Conclusion

By slightly changing the headgroup–headgroup and headgroup–water interaction of lipids in both monolayers separately, spontaneous curvature can be introduced in a membrane. Because of this spontaneous curvature, shape changes are induced which minimize the free energy of the system. Flat periodic membranes become curved and for vesicles, depending on the sign and magnitude of the spontaneous curvature, a wide variety of vesicle shapes is obtained. Small changes in the interactions, which in nature could be a result of domains with slightly different lipids or slightly different inner and outer environments, e.g., pH or ions, thus can have a tremendous influence on the vesicle shapes. Our simulations have been performed on relatively small vesicles, but since the relevant parameter c_0 is linear in the vesicle size R_0 , this influence on the vesicle shape holds even stronger for larger vesicles. The shapes found in our molecular dynamics simulations compare well with experimental as well as theoretically predicted shapes, but our simulations also show some differences and moreover allow the study at a molecular level. However, to be able to fully predict the shapes of our relatively small vesicles, the theoretical models should be extended to include explicitly the bilayer thickness. Our simulations showed that spontaneous curvature arises from the positioning of domains with the different lipid types opposite to each other in the two monolayers.

Acknowledgment. We thank Koen Pieterse, Peter Spijker, and Sander Smeijers, as without their prior work these simulations could not have been done. We also thank our colleagues from the Mathematics department and Eurandom, Mark Peletier, Remco van der Hofstad, and Maarten van Wieren for many fruitful discussions.

References and Notes

- (1) Tanaka, T.; Sano, R.; Yamashita, Y.; Yamazaki, M. *Langmuir* **2004**, *20*, 9526–9534.
- (2) Käs, J.; Sackmann, E. *Biophys. J.* **1991**, *60*, 825–844.
- (3) Helfrich, W. *Z. Naturforsch.* **1973**, *28c*, 693–703.
- (4) Svetina, S.; Zeks, B. *Biomed. Biochim. Acta* **1983**, *42*, 86–90.
- (5) Svetina, S.; Zeks, B. *Eur. Biophys. J.* **1989**, *17*, 101–111.
- (6) Miao, L.; Seifert, U.; Wortis, M.; Döbereiner, H.-G. *Phys. Rev. E* **1994**, *49*, 5389–5407.
- (7) Deuling, H.; Helfrich, W. *J. Phys. (Paris)* **1976**, *37*, 1335–1345.
- (8) Seifert, U.; Berndl, K.; Lipowsky, R. *Phys. Rev. A* **1991**, *44*, 1182–1202.
- (9) Baumgart, T.; Hess, S.; Webb, W. *Nature (London)* **2003**, *425*, 821–824.
- (10) Bacia, K.; Schwille, P.; Kurzchalia, T. *Proc. Natl. Acad. Sci. U.S.A.* **2005**, *102*, 3272–3277.
- (11) Markvoort, A.; Pieterse, K.; Steijaert, M.; Spijker, P.; Hilbers, P. *J. Phys. Chem. B* **2005**, *109*, 22649–22654.
- (12) Smeijers, A.; Markvoort, A.; Pieterse, K.; Hilbers, P. *J. Phys. Chem. B* **2006**, *110*, 13212–13219.
- (13) Smeijers, A.; Pieterse, K.; Markvoort, A.; Hilbers, P. *J. Phys. Chem. B* **2006**, *110*, 13614–13623.